He S *et al.* (2025)
Notulae Botanicae Horti Agrobotanici Cluj-Napoca
Volume 53, Issue 1, Article number 14148
DOI:10.15835/nbha53114148
Research Article

# Effects of different rootstocks on the growth physiology and enzyme activity of *Artemisia selengensis*

Sixiao HE[1a], Mang XIA[1b], Meizhu CHEN[1], Xiaoxiao DONG[1], Miao CHENG[1], Jingdong CHEN[1], Tianyuan XUE[1] Heping WAN[1,2], Yuanhuo DONG[1,2], Changli ZENG[1,2], Xigang DAI[1,2]*

[1]*Jianghan University, School of Life Science, Wuhan 430056, China; sx_he@foxmail.com; xiamang@stu.jhun.edu.cn; 15172514881@163.com; dong_0087@163.com; 18971227301@163.com; cjd19951226@126.com; xty99100911@163.com; wanheping@jhun.edu.cn; 13476837028@163.com; zengchangli@jhun.edu.cn; xg_dai@163.com (*corresponding author)*
[2]*Hubei Engineering Research Center for Protection and Utilization of Special Biological Resources in the Hanjiang River Basin, Wuhan 430056, China*
[a,b]*These authors contributed equally to the work*

## Abstract

In this experiment, wild-type *Artemisia selengensis*, *Chrysanthemum*, *Artemisia annua* and mugwort were used as rootstocks, while cultivated *A. selengensis* served as the scion. Cleft grafting was identified as the most effective method. The highest survival rate was observed when wild-type *A. selengensis* was used as the rootstock, reaching 92.5% on the 12th day post-grafting, with quicker callus formation than in other combinations. The combination of wild-type *A. selengensis* rootstock and cultivated *A. selengensis* scion demonstrated the greatest grafting compatibility, whereas the pairing of cultivated *A. selengensis* with chrysanthemum showed the lowest. During the healing phase, analysis revealed that in compatible graft combinations, soluble sugar levels increased, with a significant rise in soluble protein levels. Following callus formation, levels of superoxide dismutase (SOD), peroxidase (POD), and phenylalanine ammonia-lyase (PAL) declined. Hence, soluble sugars, SOD, POD, and PAL may act as indicators of grafting compatibility in *A. selengensis*. Weekly elongation measurements from 21 to 49 days post-grafting indicated that combinations rooted in chrysanthemum exhibited markedly greater elongation from 35 to 49 days than other pairs. Comparisons of soluble proteins, sugars, vitamin C, and flavonoids in the scion on days 49, 70, and 91 post-grafting with those in ungrafted plants suggested that different rootstocks differentially influenced nutrient and metabolite accumulation in *A. selengensis*. These findings suggest that future research could explore the mechanisms underlying these changes during the grafting process. Integrating molecular biology and metabolomics techniques will aid in elucidating specific regulatory mechanisms affected by grafting in *Artemisia* species, potentially enhancing the content of nutrients or bioactive compounds. This could provide theoretical support for biopharmaceutical applications and propose new methods for improving the quality of *Artemisia* germplasm resources.

***Keywords:*** *Artemisia selengensis*; grafting; growth nutrients; graft combination; growth physiology

*Received: 26 Sep 2024. Received in revised form: 28 Nov 2024. Accepted: 12 Feb 2025. Published online: 11 Mar 2025.*
From Volume 49, Issue 1, 2021, Notulae Botanicae Horti Agrobotanici Cluj-Napoca journal uses article numbers in place of the traditional method of continuous pagination through the volume. The journal will continue to appear quarterly, as before, with four annual numbers.

## Introduction

*Artemisia selengensis*, a member of the *Asteraceae* family, is valued as a specialty vegetable. Its tender and crisp stems are primarily consumed (Wang et al., 2020). Renowned for its distinctive flavor and rich nutritional content, *A. selengensis* is widely appreciated not only as a popular culinary ingredient but also for its extensive applications in medicine, healthcare, and the chemical industry (Lu *et al*., 2014).

In recent years, the production of *A. selengensis* has become increasingly mechanized and large-scale. However, the plant faces challenges in the central Yangtze River region, where issues such as difficulties with flowering, low pollen viability, and reliance on cutting propagation have led to reduced genetic diversity and variety degradation. This situation has significantly hampered breeding research. Currently, the market offers only a few cultivated varieties, such as 'Kunming Dabaiye', 'Nanjing Daye', 'Yunnan Lvgan', 'Kunming Summer' *Artemisia*, 'Nanjing Winter' *Artemisia*, and some domesticated wild types. In Hubei, the principal cultivated varieties are limited to 'Nanjing 6-Daye Qing Lihao' and 'Yunnan Lvgan Lihao' (Fu *et al*., 2016). The long-term dependence on cutting propagation has caused severe quality degradation, resulting in subpar taste and quality in some cultivated varieties. Therefore, there is an urgent need to develop new, high-quality varieties of *A. selengensis*.

Grafting, a form of vegetative propagation that involves asexual reproduction, has been practiced in Chinese horticulture for over 4,000 years. During this process, new parenchyma cells are produced at the junction between the rootstock and scion, differentiating into callus tissue that quickly merges and interlocks to form a single, unified plant (Yildirim *et al*., 2017). Different grafting techniques are applied based on the location of the parenchyma cells: for woody plants like roses and grapes, the vascular cambium must be perfectly aligned, whereas for herbaceous plants such as rapeseed, watermelon, and cucumber, the cortex layers must be properly matched (Kumar *et al*., 2023). The main grafting methods include cleft, approach, side, and splice grafting, with the choice of technique depending on the specific rootstock-scion combination. Furthermore, the selection of the appropriate rootstock can significantly enhance the plant's secondary metabolism. For example, grapevine grafting has demonstrated that the right rootstock can upregulate genes related to anthocyanin synthesis in the scion, thus accelerating fruit ripening (López Serrano *et al*., 2022), and improving salt tolerance in tomatoes (Lupp *et al*., 2024).

In China, wild *A. selengensis* germplasm resources are abundant and widely distributed across 19 provinces, including Heilongjiang, Shandong, Sichuan, Yunnan, and Guizhou. These varieties exhibit strong resistance and high levels of active substances. Extensive research on Artemisia species such as *A. selengensis*, *Artemisia annua, Artemisia argyi*, and chrysanthemum spans pharmacology, clinical medicine, food development, and personal care products (Borgo *et al*., 2024). *Artemisia annua, Artemisia argyi*, and chrysanthemum are particularly valued as medicinal and edible plants due to artemisinin's notable contributions to malaria treatment, which has heightened interest in Artemisia species (Chen *et al*., 2022). Research in traditional Chinese medicine is also thriving, with Artemisia species frequently used as rootstocks to effectively increase the biomass and physiological activity of grafted chrysanthemums (Li *et al*., 2022). This study aims to graft cultivated *A. selengensis* onto *Artemisia annua, Artemisia argyi*, chrysanthemum, and wild-type *A. selengensis* to examine changes in nutrient enzymes during grafting and assess various nutritional indicators of the grafted *A. selengensis*. This research will explore the grafting compatibility between *Artemisia* species and chrysanthemum, aiming to verify the feasibility of obtaining high-quality *A. selengensis* germplasm resources through grafting and to provide a theoretical foundation for subsequent research on molecular mechanisms and the development of new *Artemisia* germplasm resources.

## Materials and Methods

*Experimental materials*

The experiment was conducted in an Artemisia species nursery. Grafting occurred from March 1 to March 8, with nighttime temperatures ranging from 5 °C to 13 °C and daytime temperatures between 17 °C and 24 °C. Healthy, pest-free, and disease-free *Artemisia selengensis* plants (cultivar No. 2) from the Asteraceae nursery were selected as scions. *Artemisia annua*, *Artemisia argyi*, chrysanthemum, and wild-type *Artemisia selengensis* (L5) served as rootstocks. The scion-rootstock combinations are detailed in Table 1.

**Table 1.** experimental materials

| Scion | Rootstock | Scion abbreviation | Scion-rootstock combinations abbreviation |
|---|---|---|---|
| *Artemisia selengensis* cultivar No. 2 | *Artemisia annua* (Q1) | L1 | L1Q1 |
| | *Artemisia argyi* (A2) | L2 | L2A1 |
| | Chrysanthemum (J1) | L3 | L3J1 |
| | wild-type *Artemisia selengensis* (L5) | L4 | L4L5 |

*Grafting experiment with Artemisia selengensis*

Scions of *Artemisia selengensis,* with stem diameters of 0.6 to 1 cm, were prepared by cutting 9-10 cm from the stem tips and removing excess leaves. Compact, healthy rootstocks were selected, and cuts were made 6-10 cm above the root base. The cleft grafting method was employed to graft the scions onto various rootstocks. Graft sites were secured with plastic film to ensure proper alignment of the cambial layers. After grafting, the plants were placed in shaded, well-ventilated areas. Before the grafts healed, the pots were watered every two days, and the scions were misted daily to maintain leaf moisture. Once the grafts had healed, watering frequency was reduced to every three days (Figure 1). Four grafting combinations were tested, with 30 plants per combination, resulting in 120 plants per experimental unit. Three replicate units were established, each in a distinct shaded and ventilated location within the experimental site. Scion survival was assessed by the emergence of buds from the scion tips 12 days after grafting. The survival rate was calculated as follows: Survival rate (%) = (Number of scions with bud emergence at 12 days / Total number of grafted plants) × 100.

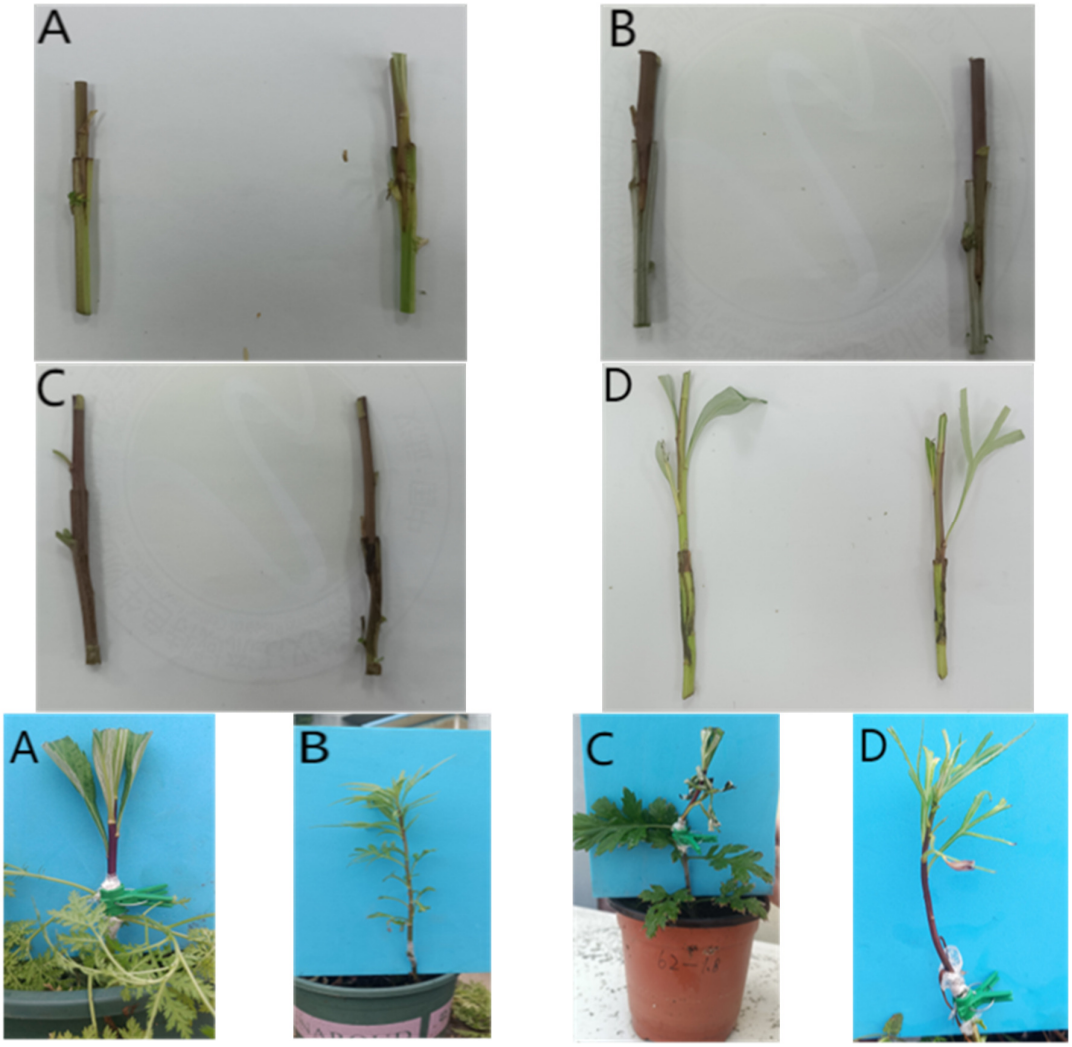


**Figure 1.** (A) *Artemisia annua* was used as the rootstock and *Artemisia selengensis* cultivar No. 2 was used as the scion for grafting (L1Q1). (B) *Artemisia argyi* was used as the rootstock and *Artemisia selengensis* cultivar No. 2 was used as the scion for grafting (L2A1). (C) Chrysanthemum is used as the rootstock and *Artemisia selengensis* cultivar No. 2 was used as the scion for grafting (L3J1). (D) wild-type *Artemisia selengensis* was used as the rootstock and *Artemisia selengensis* cultivar No. 2 was used as the scion for grafting (L4L5).

*Assessment of physiological indicators at the graft union*

Samples were collected at 2, 4, 6, 8, 10, and 12 days after grafting. For each sampling date, two grafted plants from each unit were selected, totaling six plants per grafting combination. The graft union site was examined for healing, photographed, and recorded. The scion part was then cut and preserved with a 3 cm segment. Initially, these samples were frozen in liquid nitrogen, then placed in sealed bags, and stored at -80 °C. After the 12-day sampling period, soluble sugars were measured using the anthrone colorimetric method (Rondel *et al*., 2013). Take 0.2 g of the sample and extract it into a solution using distilled water. Then, add the anthrone reagent to the solution. Place the test tube in a constant-temperature water bath and heat for 10-15 minutes, observing any color changes. After cooling, measure the absorbance of the sample solution at 620 nm using a spectrophotometer. By measuring the absorbance, use the standard curve to calculate the soluble sugar content in the sample.

Soluble proteins were determined using the Coomassie Brilliant Blue G-250 method (Jones *et al*., 1989). Initially, 0.2 grams of the sample were accurately weighed, thoroughly rinsed, and positioned within a pre-cooled mortar. Sequentially, 1.6 mL of chilled 50 mM phosphate buffer at pH 7.8 was added in increments of 0.6 mL, 0.5 mL, and 0.5 mL. The sample was then ground into a uniform slurry on ice and transferred to a centrifuge tube, where it was centrifuged at 4 °C and 12,000 g for 20 minutes to separate the supernatant, yielding a crude protein extract. To quantitatively assess protein concentration, standard solutions of proteins like BSA were prepared at defined concentrations to establish a calibration curve. The sample was then mixed with an equal volume of Coomassie Brilliant Blue G-250 dye and incubated at ambient temperature for 30 minutes, leading to a color shift from red to blue as the dye bound to the proteins. The reaction's absorbance was measured at 595 nm using a spectrophotometer, which is directly proportional to the protein concentration. This relationship enabled the plotting of a standard curve based on known concentrations and their corresponding absorbance values, facilitating the determination of the sample's protein concentration via this curve.

POD activity was quantified using the guaiacol method (Fijalkowski *et al*., 2020). 2 g of the sample were placed into a mortar, to which 5.0 mL of extraction buffer was added. The mixture was ground to form a consistent slurry under ice-cold conditions and subsequently centrifuged at 12,000 × g for 30 minutes at 4 °C. The supernatant, constituting the enzyme extract, was then preserved at a low temperature for further analysis. In a subsequent step, a test tube was prepared with 3.0 mL of 25 mM guaiacol and 0.5 mL of the enzyme extract. Addition of 200 μL of 0.5 M $H_2O_2$ initiated the reaction, with immediate mixing and simultaneous timer activation. This mixture was then transferred into a cuvette in a spectrophotometer's sample chamber, with distilled water serving as the reference. Absorbance was first recorded at 470 nm after 15 seconds and subsequently every minute for six points in total, with each measurement conducted in triplicate. These data points were used to plot absorbance against time, from which the initial linear section was used to calculate the rate of change in absorbance per minute (ΔOD470). The POD activity is expressed as ΔOD470 per gram of fresh weight of the sample.

Catalase (CAT) activity was quantified using the potassium permanganate titration method (Pang *et al*., 2020). Weigh 2 g of the sample and add a small amount of phosphate buffer (pH 7.8). Grind the sample into a homogeneous slurry and transfer it to a 25 mL volumetric flask. Wash the mortar with the same buffer and transfer the washings to the volumetric flask. Then, fill the flask to the mark with the same buffer solution. Centrifuge the mixture at 4000 rpm for 15 minutes and collect the supernatant, which serves as the crude CAT extract. Prepare four 50 mL conical flasks (two for measurement and two as controls). Add 2.5 mL of the enzyme extract to the measurement flasks and 2.5 mL of heat-inactivated enzyme solution (boiled) to the control flasks. Then, introduce 2.5 mL of 0.1 mol/L $H_2O_2$ to all flasks. Start the timer immediately after adding the $H_2O_2$, and incubate the flasks in a 30 °C water bath for 10 minutes. Following incubation, promptly add 2.5 mL of 10% $H_2SO_4$ to each flask. Titrate the reaction mixture with 0.1 mol/L $KMnO_4$ standard solution until a persistent pink color develops, remaining stable for 30 minutes. CAT activity is computed using the formula below:

$$\text{Catalase activity} = \frac{(A - B) \times V_T}{W \times V_S \times 1.7 \times t}$$

- A is the volume of $KMnO_4$ used in the control titration
- B is the volume of $KMnO_4$ used in the enzyme reaction titration
- $V_T$ is the total volume of the enzyme extract
- $V_S$ is the volume of enzyme solution used in the reaction
- W is the fresh weight of the sample
- t is the reaction time

SOD activity was determined using the nitroblue tetrazolium method (Durak *et al*., 1993). Weigh 0.5 g of the sample and add an adequate amount of ice-cold phosphate buffer to form a homogeneous slurry.

Centrifuge the slurry at 12,000 rpm for 15 minutes to obtain the SOD extract. Organize the experiment into two groups: a sample group (with enzyme solution) and a control group (with heat-inactivated enzyme solution or without enzyme). Add 2 mL of phosphate buffer, 0.1 mM NBT solution, xanthine solution, and xanthine oxidase solution to the reaction tubes and mix thoroughly. Introduce an appropriate volume of the SOD extract into the reaction tubes. Start the timer and incubate the tubes in a 30 °C water bath for 10 minutes. Subsequently, add 0.1 M $Na_2CO_3$ solution to neutralize and halt the reaction. Measure the absorbance of the reaction mixture at 560 nm using a spectrophotometer. Record the absorbance values for both the sample and the control groups. Calculate the SOD activity by assessing the difference in absorbance between these two groups.

$$\text{SOD activity} = \frac{(A_{\text{control}} - A_{\text{sample}})}{T}$$

PAL activity was measured using Kováčik et al.'s method (Kováčik *et al*., 2012). Weigh 0.5-1 g of the sample and add an appropriate amount of ice-cold phosphate buffer to produce a homogeneous slurry. Centrifuge the slurry at 12,000 rpm for 15 minutes and collect the supernatant, the PAL extract. In a test tube, combine 3 mL of phosphate buffer, 0.2 mL of L-phenylalanine solution, and 0.1 mL of the PAL extract. Incubate the reaction mixture in a 30 °C water bath for 60 minutes. To terminate the reaction and neutralize the solution, add 1 mL of 1 M $Na_2CO_3$. Measure the absorbance of the reaction mixture at 290 nm using a spectrophotometer. Record the absorbance for both the sample and control groups. Calculate the PAL activity by determining the difference in absorbance between the two groups.

$$\text{PAL Activity (U)} = \frac{\Delta A \times V_{total}}{\epsilon \times l \times W \times t}$$

- ΔA is the change in absorbance
- $V_{total}$ is the total volume of the reaction mixture
- ε is the molar absorption coefficient of cinnamic acid at 290 nm
- l is the path length of the cuvette
- W is the fresh weight of the sample
- t is the time of the reaction

*Measurement of scion elongation*

On day 21, two scions from each unit were selected to measure their initial length. This measurement was repeated across three replicate units. Scions were marked, and subsequent measurements were taken on days 28, 35, 42, and 49. The elongation rate was calculated based on the length measurements taken over the four-week period.

*Measurement of nutritional content in Artemisia selengensis*

On days 49, 70, and 91 post-grafting, three scion plants were sampled from each unit. A total of nine scions per grafting combination were collected and placed in corresponding envelopes. The fresh stems and leaves were analyzed for various nutritional indicators: Vitamin C content was measured using the 2,6-dichlorophenolindophenol titration method (Aguiar *et al*., 2017). Soluble protein levels were determined using the Coomassie Brilliant Blue method (Jones *et al*., 1989). Soluble sugar content was assessed using the anthrone colorimetric method (Rondel *et al*., 2013). Flavonoids were quantified by drying and grinding the stems and leaves, followed by measurement using the sodium nitrite colorimetric method (Matić *et al*., 2017). The control group (CK) consisted of the non-grafted cultivated type 2.

*Data analysis*

Data analysis was performed using SPSS 18.0 for statistical processing and Origin 2021 for graphing.

## Results

*Healing conditions in different grafting combinations*

The compatibility between rootstock and scion markedly influences the rate of graft healing. Examination of healing processes across diverse graft combinations shows that callus development is most prompt in grafts involving both cultivated and wild Artemisia species. Specifically, the L1Q1 and L2A1 combinations initiate callus formation on days 6 and 8, respectively. The L3J1 pairing exhibits callus development by day 10. Notably, by day 14, the L4L5 pair demonstrates superior healing (Table 2).

**Table 2.** Healing conditions in different grafting combinations

| Scion-rootstock combinations abbreviation | Callus formation time (d) | Number of plants with callus formation at 14 days (%) |
|---|---|---|
| L1Q1 | 6 | 85 |
| L2A1 | 8 | 79 |
| L3J1 | 10 | 70 |
| L4L5 | 4 | 94 |

*Survival outcomes across grafting combinations*

When grafting Artemisia as the scion with four distinct rootstocks, the survival outcomes at 12 days post-grafting are detailed in Figure 2. The L4L5 graft shows an optimal survival rate of 92.5%, in contrast to the L3J1, which records the lowest at 67.5%. Notably, the survival rate for L4L5 significantly surpasses those observed in other combinations.

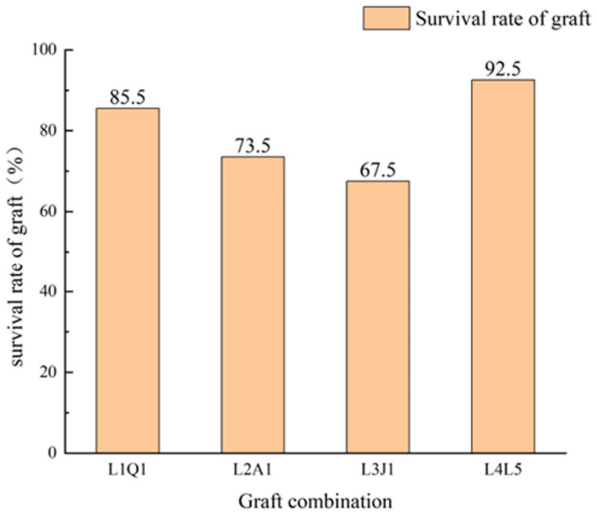


**Figure 2.** Survival rates of different grafting combinations

*Physiological and biochemical changes at the grafting interface trends in soluble sugar levels*

Figure 3 illustrates the trends in soluble sugar levels within various rootstock-scion combinations throughout the graft healing phase. This metric suggests a consistent consumption of soluble sugars during

initial healing stages. In the L1Q1 graft, soluble sugar levels diminish to 1.44%, a 76.29% decrease from day 2 by day 12. Similarly, for L2A1, levels fall to 0.90%, down by 85.09% from day 2. The L3J1 combination sees a continual drop to 0.31%, reflecting a 95.27% reduction from day 2. Contrastingly, the L4L5 combination shows a decline in soluble sugar to 2.63% by day 10, a reduction of 53.78% from day 2, followed by a rise to 3% between days 10 and 12.

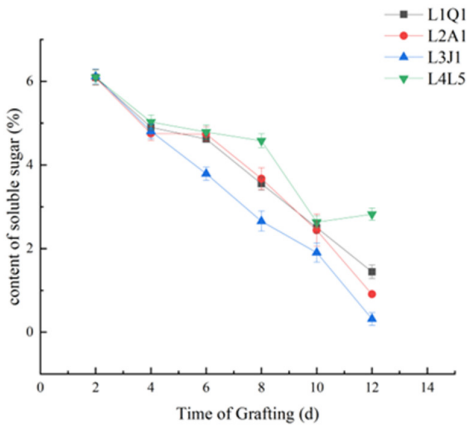


**Figure 3.** Dynamic changes in soluble sugar content at the grafting interface of different combinations

*Fluctuations in soluble protein levels*

Figure 4 elucidates the variable levels of soluble protein content across different grafting combinations. In the L4L5 combination, soluble protein levels drop to 1.96 mg/g over the initial six days, constituting 60.25% of the initial measurement. Subsequently, these levels rise to 2.75 mg/g by day 12, marking a 28.68% increase. The L1Q1 pairing experiences a steady reduction in soluble protein to 1.03 mg/g by day 10, followed by a rise to 1.80 mg/g by day 12, an uptick of 19.09%. For the L2A1 combination, there is a decrease in soluble protein content to 1.27 mg/g by day 10, which is 52% of the original level, then an increment to 1.68 mg/g by day 12, an increase of 10.3%. The L3J1 combination observes a reduction to 2.16 mg/g by day 4, a 23.6% decrease from the initial level. This is followed by a temporary increase to 2.71 mg/g by day 6, and a subsequent fall to 1.31 mg/g by day 12, a decline of 29.65%.

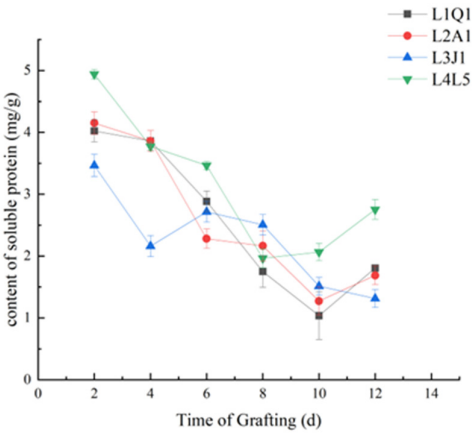


**Figure 4.** Dynamic changes in soluble protein content at the grafting interface of different combinations

*Temporal variations in phenylalanine ammonia lyase (PAL)) levels*

PAL, predominantly localized in vascular tissues and epidermal cells, facilitates cell differentiation and lignification by participating in lignin production. Figure 5 depicts the fluctuations in PAL levels across various rootstock-scion pairings, characterized by an initial decrease followed by subsequent increases. In the L4L5 pairing, PAL content initially drops by 29.26% to 58.69 $Ug^{-1}$ $min^{-1}$ between days 2 and 6, then ascends to 93.26 $Ug^{-1}$ $min^{-1}$ by day 10, and finally decreases by 15.6% by day 12. The L1Q1 combination shows a rise in PAL to 81.71 $Ug^{-1}$ $min^{-1}$ by day 4, a fall to 63.35 $Ug^{-1}$ $min^{-1}$ by day 8 (a 22.47% reduction), and a subsequent increase to 84.50 $Ug^{-1}min^{-1}$ by day 12. For the L2A1 combination, PAL reduces to 45.68 $Ug^{-1}$ $min^{-1}$ by day 8 (a decrease of 30.59%) and then climbs to 59.42 $Ug^{-1}$ $min^{-1}$ by day 12. The L3J1 combination exhibits a 50.07% decrease to 40.76 $Ug^{-1}$ $min^{-1}$ by day 8, followed by a rise to 55.88 ± 2.79 $Ug^{-1}$ $min^{-1}$ (a 36.96% increase) by day 12.

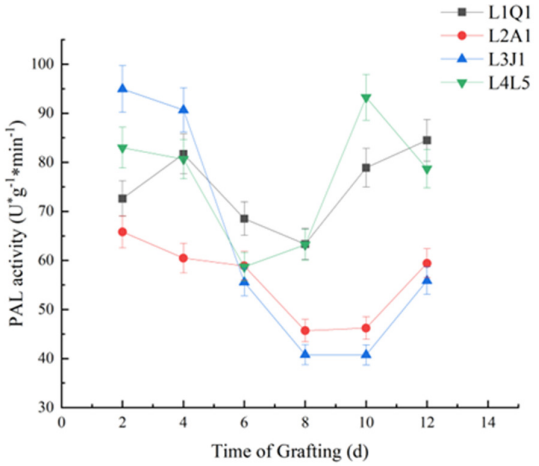


**Figure 5.** Dynamic changes in PAL content at the grafting interface of different combinations.

*Dynamic shifts in SOD levels*

The dynamics of SOD content, outlined in Figure 6, demonstrate an initial increase and subsequent decrease across all grafting combinations. For instance, the L4L5 combination shows an increase in SOD from 222.296 $Ug^{-1}$ $min^{-1}$ to 300.50 $Ug^{-1}$ $min^{-1}$ from days 2 to 6, followed by a decrease to 195.978 $Ug^{-1}$ $min^{-1}$ by day 12. In the L1Q1 combination, SOD levels ascend from 300.031 $Ug^{-1}$ $min^{-1}$ to 342.201 $Ug^{-1}$ $min^{-1}$ between days 2 and 6, then diminish to 265.379 $Ug^{-1}$ $min^{-1}$ by day 12. Similarly, for the L2A1 combination, SOD content rises from 288.978 $Ug^{-1}$ $min^{-1}$ to 338.897 $Ug^{-1}$ $min^{-1}$ over the same initial period, and subsequently decreases to 297.741 $Ug^{-1}$ $min^{-1}$ by day 12. The L3J1 combination experiences an increase from 199.035 $Ug^{-1}$ $min^{-1}$ to 298.152 $Ug^{-1}$ $min^{-1}$ throughout the 12-day period.

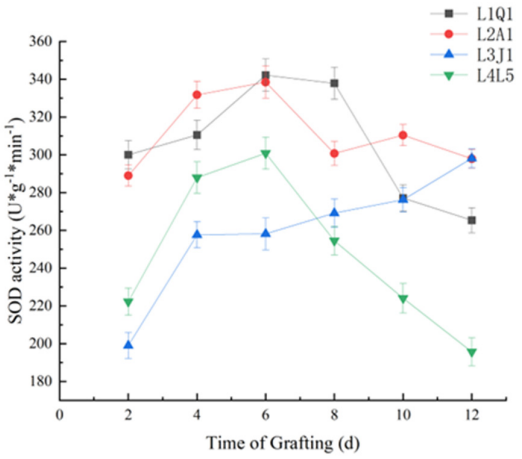


**Figure 6.** Dynamic changes in SOD content at the grafting interface of different combinations

*Temporal fluctuations in POD Levels*

As depicted in Figure 7, POD content exhibits an overall upward trend throughout the graft healing phase. In the L1Q1 pairing, POD levels steadily rise from 199.311 $Ug^{-1}$ $min^{-1}$ to 267 $Ug^{-1}$ $min^{-1}$ over a span of 10 days, marking a 1.33-fold increase. The L2A1 combination sees an ascent in POD from 216.311 $Ug^{-1}$ $min^{-1}$ to 273 $Ug^{-1}$ $min^{-1}$ by day 8, an increment of 26.41%. This is followed by a decline to 246.93 $Ug^{-1}$ $min^{-1}$ by day 10, before rebounding to 273.66 $Ug^{-1}$ $min^{-1}$ by day 12. For the L4L5 combination, an initial increase from 217.4 $Ug^{-1}$ $min^{-1}$ to 256.04 $Ug^{-1}$ $min^{-1}$ is noted from days 2 to 4, subsequently decreasing to 239.95 $Ug^{-1}$ $min^{-1}$ by day 6, and then elevating to 305.15 $Ug^{-1}$ $min^{-1}$ by day 12.

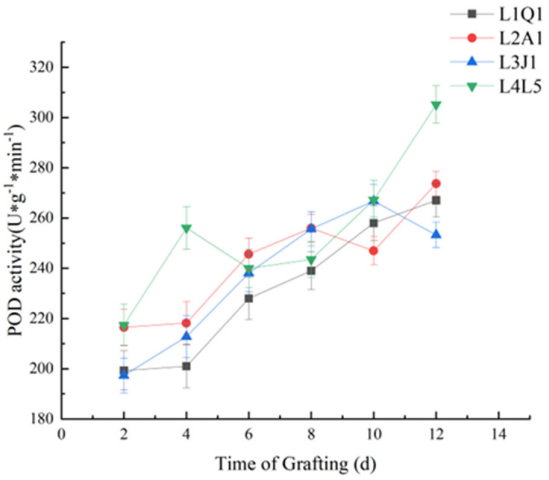


**Figure 7.** Dynamic changes in POD content at the grafting interface of different combinations

*Dynamic Changes in CAT Content*

Figure 8 illustrates that CAT content during the graft healing period follows an "M" shaped trajectory. In the L1Q1 combination, CAT levels escalate from 7.55 Ug-1 min-1 to 16.66 $Ug^{-1}$ $min^{-1}$ between days 2 and 6, then dip to 12.3 ± 0.61 $Ug^{-1}$ $min^{-1}$ between days 6 and 8. CAT then climbs to 14.4 $Ug^{-1}$ $min^{-1}$ by day 10, and finally falls to 13 $Ug^{-1}$ min-1 by day 12. In the L2A1 combination, CAT content increases from 4.72 $Ug^{-1}$ min-

$^{1}$ to 15.5 $Ug^{-1}$ $min^{-1}$ from days 2 to 6, decreases to 11 $Ug^{-1}$ $min^{-1}$ from days 6 to 8, and rises again to 18.53 $Ug^{-1}$ $min^{-1}$ by day 12. The L3J1 combination exhibits a rise in CAT from 8.5 ± 0.42 Ug-1 min-1 to 20.08 Ug-1 $min^{-1}$ from days 2 to 6, followed by a decrease to 13.16 $Ug^{-1}$ $min^{-1}$ from days 6 to 8. CAT then ascends to 17.16 ± 0.85 $Ug^{-1}$ $min^{-1}$ from days 8 to 10 and drops again to 11.53 $Ug^{-1}$ $min^{-1}$ by day 12. Meanwhile, for the L4L5 combination, CAT increases from 7.93 $Ug^{-1}$ $min^{-1}$ to 18.91 $Ug^{-1}$ $min^{-1}$ from days 2 to 6 and consistently declines to 10.53 $Ug^{-1}$ $min^{-1}$ by day 12.

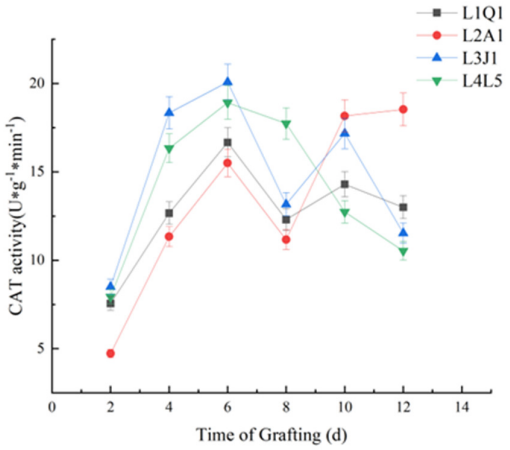


**Figure 8.** Dynamic changes in CAT content at the grafting interface of different combinations

*Effects of different rootstocks on the elongation of Artemisia selengensis scions*

From Figure 9, measurements of scion elongation began 21 days post-grafting and were conducted weekly. The results are presented in the table. Between days 21 and 28, elongation in L1Q1 was markedly higher than in L2A1, L3J1, and L4L5, although differences among L2A1, L3J1, and L4L5 were negligible during this period. From days 28 to 35, L1Q1 continued to exhibit significantly higher elongation compared to L3J1, L4L5, and L2A1, with no significant differences noted between L3J1 and L4L5. Between days 35 and 42, L3J1 demonstrated greater elongation than L2A1, which in turn was greater than that of both L1Q1 and L4L5. From days 42 to 49, elongation of L3J1 surpassed that of L1Q1, L2A1, and L4L5, with L3J1 exhibiting a significant increase of 13.7 ± 0.26 cm compared to other combinations. In the subsequent week, the unit elongation of L3J1 remained superior to that of the other combinations.

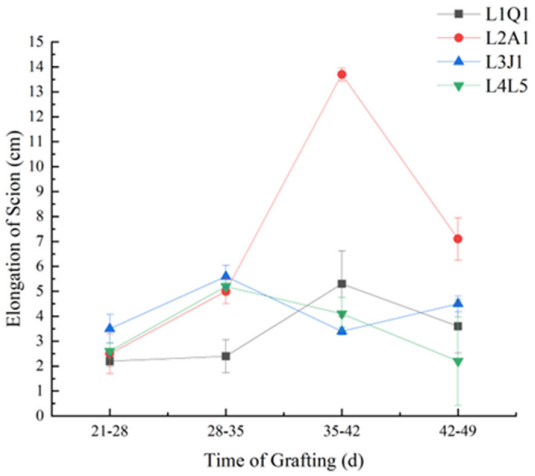


**Figure 9.** Elongation of *Artemisia selengensis* scions: effects of different rootstocks

*Investigation of the linear relationship*

In the analysis of flavonoids, soluble proteins, and soluble sugars, standard curves were constructed using various concentrations of rutin, bovine serum albumin, and sucrose, respectively. As indicated in Table 3, $R^2$ values were all above 0.99, demonstrating a strong linear relationship that satisfies the experimental requirements.

**Table 3.** Linear relationship and range of the measured components

| Components to be measured | Regression equation | Linear (μg/ml) | $R^2$ |
|---|---|---|---|
| Flavonoids | y=0.0112x+0.1129 | 0~50 | 0.9992 |
| Soluble Sugars | y=0.0023x+0.0506 | 0~100 | 0.9907 |
| Soluble Proteins | y=0.02x+0.2216 | 0~50 | 0.9901 |

*Effects of grafting with different rootstocks on the nutrient content of Artemisia selengensis changes in vitamin c and flavonoid content*

At various time points post-grafting, samples were collected from each rootstock-scion combination to assess changes in vitamin C and flavonoid content within the stems and leaves. According to Figure 10, both vitamin C and flavonoid levels were generally higher in the leaves than in the stems. Vitamin C accumulation varied among different rootstocks. On day 49, the vitamin C levels in the stems of the control group (CK, 1.19 mg/g) and L4L5 (1.86 mg/g) were notably higher than those in L1Q1, L2A1, and L3J1, with no discernible difference between CK and L4L5. In the leaves, the levels in L2A1 (3.51 mg/g), L3J1 (3.45 mg/g), L4L5 (2.89 mg/g), and CK (2.7 mg/g) exceeded those in L1Q1, with no significant variations among L2A1, L3J1, L4L5, and CK. By day 70, the vitamin C content in the stems of L2A1 was significantly greater than in L1Q1, CK, and L4L5. In the leaves, vitamin C levels in CK, L1Q1, and L2A1 surpassed those in L3J1 and L4L5. On day 91, the vitamin C levels in the leaves of L1Q1, L2A1, L4L5, and CK were substantially higher than in L3J1, with no significant differences observed in the stems.

The flavonoid accumulation also differed across various rootstock grafting combinations. On day 49, the flavonoid content in the leaves of L4L5 (134.12 mg/g) was significantly higher than in L3J1, CK, L1Q1, and L2A1. In the stems, the content in L3J1 (72.94 mg/g) exceeded that in L4L5, L1Q1, CK, and L2A1. By day 70, the flavonoid levels in the leaves of L1Q1, L2A1, and L4L5 were higher than in CK (49.63 mg/g). In the stems, L3J1's flavonoid content (51.97 mg/g) surpassed CK's (33.69 mg/g). On day 91, the flavonoid

content in the leaves of L2A1 (134.74 mg/g) was significantly greater than in L4L5, L1Q1, CK, and L3J1. In the stems, L4L5 (117.98 mg/g) had a higher flavonoid content than L1Q1 and CK.

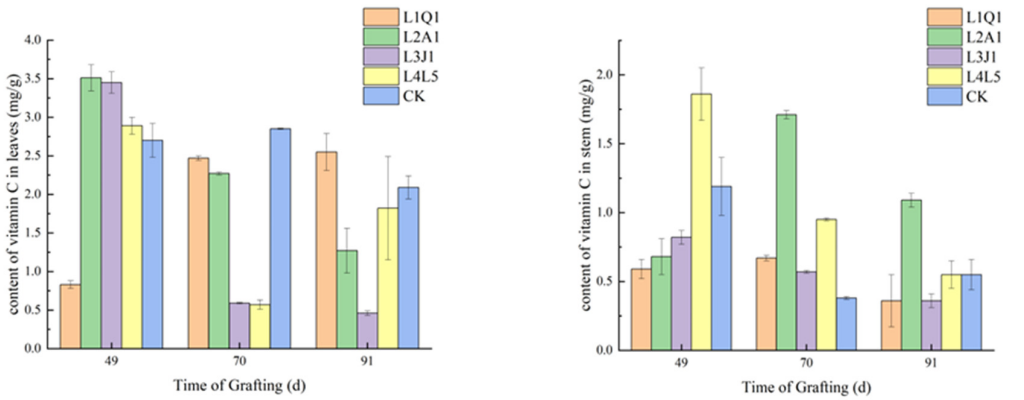


(a)

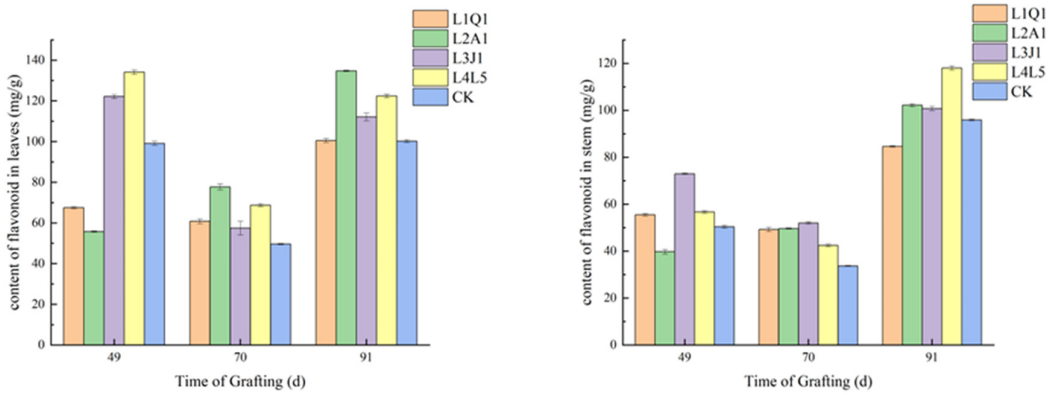


(b)

**Figure 10.** (a) Vitamin C content in the stems and leaves of *Artemisia selengensis*: Impact of different rootstocks; (b) Flavonoid content in the stems and leaves of *Artemisia selengensis*: impact of different rootstocks

*Changes in soluble protein and soluble sugar content*

As illustrated in Figure 11, the soluble protein content was generally higher in the leaves than in the stems of *Artemisia selengensis*, while the soluble sugar content was lower in the leaves than in the stems. On day 49 post-grafting, the soluble protein levels in the leaves of L4L5, CK, and L2A1 were markedly higher than in L1Q1 (10.85 mg/g), with L4L5 exhibiting notably higher levels than L3J1 (12.7 mg/g). The soluble protein levels in L4L5 stems (9.58 mg/g) also surpassed those in CK, L2A1, and L1Q1. By day 70, the soluble protein content in L2A1 leaves reached 12.93 mg/g, significantly exceeding that in CK, L3J1, and L1Q1, and in L2A1 stems, it was 8.62 mg/g, also significantly higher than in L1Q1, L4L5, CK, and L3J1. On day 91, the soluble protein content in L2A1 leaves was 11.89 mg/g, higher than that in L1Q1, L4L5, CK, and L3J1, and in L2A1 stems, it was 8.75 mg/g, again exceeding that in L1Q1, CK, and L3J1.

The regulation of soluble sugar synthesis displayed variability across different rootstock grafting combinations. On day 49, the soluble sugar levels in the leaves of CK and L3J1 were significantly higher than those in L1Q1 and L2A1. The soluble sugar content in L3J1 stems stood at 11.28%, considerably higher than in L4L5, L1Q1, CK, and L2A1. By day 70, the soluble sugar levels in L3J1 leaves were 1.55%, significantly

surpassing those in L4L5 and L1Q1. The soluble sugar levels in L4L5 stems were 10.79%, significantly higher than in L4L5, L1Q1, CK, and L2A1. On day 91, the soluble sugar levels in L1Q1 and L4L5 leaves were significantly higher than those in L2A1, CK, and L3J1, and in the stems of L1Q1, L3J1, and CK, they were higher than in L2A1 and L4L5.

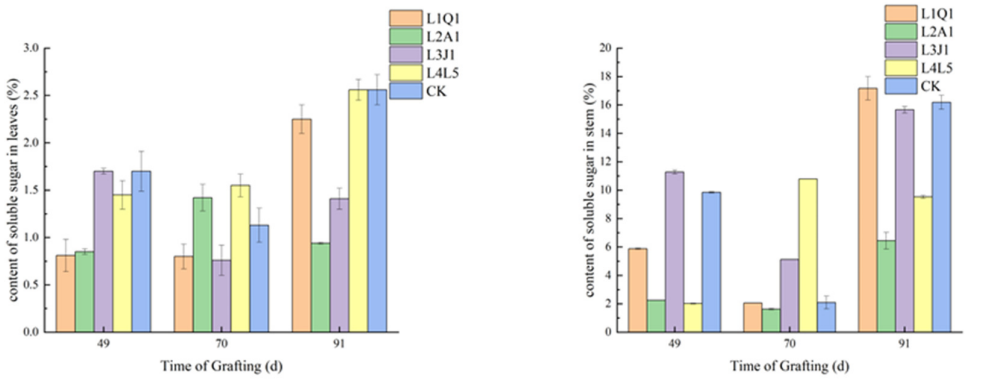


(a)

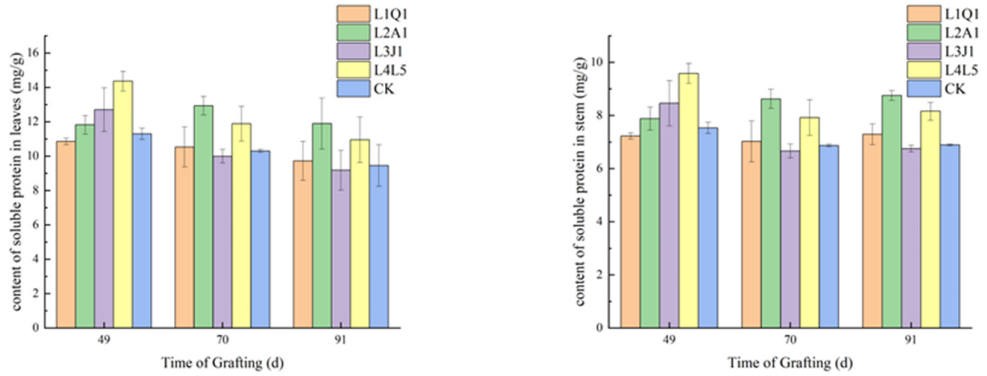


(b)

**Figure 11.** (a) Soluble sugar content in the stems and leaves of *Artemisia selengensis*: Influence of different rootstocks; (b) Soluble protein content in the stems and leaves of *Artemisia selengensis*: Influence of different rootstocks

## Discussion

Grafting introduces a novel breeding technique for *Artemisia selengensis*, which has primarily utilized cutting propagation. Although grafting is common in other plant species, studies on *A. selengensis* are limited. In this study, wedge grafting was utilized, as it is more efficient and provides a more secure junction than other methods. This secure connection reduces the leakage of phenolic compounds and polyphenol oxidase from the cut surfaces, which could otherwise enhance oxidation, lead to protein aggregation at the wound site, and hinder growth (Rashedy *et al*., 2023). Post-grafting, varied enzymatic and nutritional shifts trigger physiological and biochemical responses that enhance cell differentiation and callus formation, ultimately resulting in plant development. Soluble sugars supply essential materials and energy for cell division and differentiation, while proteins provide nitrogen for tissue structure. Both serve as signaling molecules to facilitate communication between grafted cells. However, post-grafting, some soluble sugars, proteins, and phenolic compounds are lost through wound exudate, while the remaining soluble sugars aid in regulating osmotic balance in protoplasts

and supplying energy for cell division and differentiation (Carmach *et al*., 2023). Other factors influencing grafting success include the phenological stage and the compatibility between the scion and rootstock (Calvente *et al*., 2023). This experiment was conducted in March, coinciding with the peak vegetative growth phase of Asteraceae plants, which facilitates the healing of grafted areas. The genetic relationship between the rootstock and scion is directly related to grafting success. Saithip Thippan *et al*. (2024) assessed early-stage durian graft compatibility using histological and biochemical markers.

SOD, POD, and CAT are integral to the plant's antioxidant enzyme system. SOD facilitates the conversion of superoxide radicals into hydrogen peroxide ($H_2O_2$), while CAT and POD assist in decomposing $H_2O_2$ into oxygen and water. These enzymes are crucial for maintaining a dynamic balance, scavenging free radicals, resisting oxidative stress, and mitigating damage from environmental stressors (Liu *et al*., 2023). In this study, the activity of all three enzymes was observed to increase during the initial stages of grafting due to the accumulation of reactive oxygen species (ROS) and free radicals at the graft site. These ROS contribute to the formation of a protective barrier at the wound site, preventing pathogen contamination, and participate in oxidative chain reactions within the cells (Shehata *et al*., 2023). SOD activity increased in all combinations from days 2 to 6 post-grafting. In combinations L4L5 and L1Q1, SOD activity declined from days 6 to 12, while in L3J1, it continued to rise, indicating an earlier clearance of free radicals in L4L5 and L1Q1 compared to L3J1. POD, working alongside CAT, plays a pivotal role in breaking down $H_2O_2$ and enhancing resistance to oxidative damage. It also promotes lignin accumulation, which supports vascular bundle elongation and development (Arezoo *et al*., 2024). Throughout the experiment, CAT activity increased across all combinations from days 0 to 6, whereas POD activity continued to rise through day 12, aiding callus formation and vascular regeneration. CAT activity in L4L5 showed a decline from days 6 to 12, signaling the commencement of healing, consistent with prior observations. Other combinations exhibited an "M-shaped" trend in CAT activity, indicative of its dual role in free radical scavenging and cell wall formation post-grafting.

PAL is critical for the generation and differentiation of callus cells during graft healing (Gajjar *et al*., 2023). The experiment revealed a fluctuating trend in PAL activity, initially decreasing as the plants repaired mechanical damage without forming callus tissue, then increasing as cell differentiation and callus formation commenced. Higher PAL levels are beneficial for plant tissue growth. In L4L5, PAL activity began increasing on day 6, while in L3J1 and L2A1, it rose on day 10. PAL levels in L1Q1 continued to ascend from days 8 to 12, marking the onset of callus formation. Similar patterns were observed in tea tree grafting experiments, where PAL activity increased during early callus formation and decreased once healing was complete. In this context, PAL serves as a useful indicator of graft compatibility.

Different rootstocks significantly affect the nutritional content of grafted plants. For instance, Chen Zhaofang *et al*. (2022) demonstrated that sour orange rootstocks increase total flavonoid content in Tarocco blood oranges. Similarly, grafting various sweet pepper varieties enhanced vitamin C and β-carotene levels (Garcia *et al*., 2023). In this study, the analysis revealed that nutrient and secondary metabolite contents varied through different growth stages in *A. selengensis* grafted onto diverse rootstocks. Comparative analysis between grafted and non-grafted *A. selengensis* indicated a significant impact of the rootstock on nutritional content. Specifically, using wild-type *A. selengensis* and cultivated varieties as rootstocks resulted in higher soluble protein content in the stems and leaves of grafted plants on days 70 and 91 post-grafting. When chrysanthemum served as the rootstock, soluble sugar content in the stems of grafted plants was higher than in self-rooted plants on day 49, and using wild-type *A. selengensis* as the rootstock led to higher soluble sugar content on day 70. Additionally, when A. annua was utilized as the rootstock, the vitamin C content in the stems on day 70 was significantly greater than in self-rooted plants. Regarding flavonoid content, rootstocks from the Asteraceae family had a considerable impact on cultivated *A. selengensis*. Using chrysanthemum and wild-type *A. selengensis* as rootstocks yielded significantly higher flavonoid content in the stems and leaves on day 49. Similarly, *A. annua* as the rootstock resulted in higher flavonoid content in the leaves on days 49 and 70. Fluctuations in soluble sugar, protein, vitamin C, and flavonoid contents are influenced by plant growth

stage, sampling time, and environmental conditions. This study employed three sampling times to reduce geographic and climatic interference, highlighting differences among graft combinations. Further research is required to explore how grafting influences other nutritional components in *A. selengensis*.

## Conclusions

In this study, the analysis of soluble protein, soluble sugars, vitamin C, and flavonoids in grafted scions and non-grafted *Artemisia selengensis* revealed that different rootstocks significantly influence the accumulation of nutrients and metabolites. These results provide a theoretical basis for further investigation into the molecular mechanisms involved. Future research could employ advanced techniques like grafting to extend the growth cycle of *A. selengensis*, enhance resource efficiency, and support sustainable agricultural practices. Given the medicinal and edible qualities of *A. selengensis*, these findings not only advance basic plant biology but also offer theoretical insights for the commercial cultivation and production of plant-based medicines.

## Authors' Contributions

Under supervision by XD, MX and SH performed sample preparation and data analysis. XD, MC and MC participated in the data survey. JC and TX conducted proofreading of the paper. HW and YD provided the experimental methods. CZ and XD provided project funding. All authors have read and agreed to the published version of the manuscript.

**Ethical approval** (for researches involving animals or humans)

Not applicable.

## Acknowledgements

We would like to thank the reviewers for their helpful comments on the original manuscript. This research was funded by the Key research and development project of Hubei Province (2022BBA0064,2021BBA097); the General Program of Hubei Natural Science Foundation (2022CFB640), and the Research Fund of Jianghan University (Grant No. 2022XKZX17).

## Conflict of Interests

The authors declare that there are no conflicts of interest related to this article.

## References

Abad MJ, Bedoya LM, Apaza L, Bermejo P (2012). The *Artemisia* L. genus: a review of bioactive essential oils. Molecules 17(3):2542-66. *https://doi.org/10.3390/molecules17032542*

Aguiar-Oliveira E, da Silva TL, Mazalli MR, Kamimura ES, Maldonado RR (2017). Comparison between titrimetric and spectrophotometric methods for quantification of vitamin C. Food Chemistry 224:92-96. *https://doi.org/10.1016/j.foodchem.2016.12.052*

Amri R, Font I Forcada C, Giménez R, Pina A, Moreno MÁ (2021). Biochemical characterization and differential expression of PAL genes associated with "translocated" peach/plum graft-incompatibility. Frontiers in Plant Science 622578-622578. *https://doi.org/10.3389/fpls.2021.622578*

Arezoo J, Ganji EM, Ali M (2024). Early detection of graft incompatibility in sweet cherry by internode association and callus fusion techniques. Plant Cell Tissue and Organ Culture 156(2):47. *https://doi.org/10.1007/S11240-023-02663-8*

Borgo J, Wagner MS, Laurella LC, Elso OG, Selener MG, Clavin M, ... Sülsen VP (2024). Plant extracts and phytochemicals from the asteraceae family with antiviral properties. Molecules 29(4):814. *https://doi.org/10.3390/molecules29040814*

Calvente MM, Ferreira LT, Eurya EK, Paulo M (2024). Plant grafting: maximizing beneficial microbe-plant interactions. Rhizosphere 29100825. *https://doi.org/10.1016/j.rhisph.2023.100825*

Carmach C, Castro M,Peñaloza P, Guzmán L, Marchant MJ, Valdebenito S, Kopaitic I (2023). Positive effect of green photo-selective filter on graft union formation in tomatoes. Plants (Basel) 12(19):3402. *https://doi.org/10.3390/plants12193402*

Chen B, Li C, Chang G, Wang H (2022). Dihydroartemisinin targets fibroblast growth factor receptor 1 (FGFR1) to inhibit interleukin 17A (IL-17A)-induced hyperproliferation and inflammation of keratinocytes. Bioengineered 13 (1):1530-1540. *https://doi.org/10.1080/21655979.2021.2021701*

Chen Z, Deng H, Xiong B, Li S, Yang L, Yang Y, ... Wang Z (2022). Rootstock effects on anthocyanin accumulation and associated biosynthetic gene expression and enzyme activity during fruit development and ripening of blood oranges. Agriculture 12(3):342. *https://doi.org/10.3390/agriculture12030342*

Durak I, Yurtarslanl Z, Canbolat O, Akyol O (1993). A methodological approach to superoxide dismutase (SOD) activity assay based on inhibition of nitroblue tetrazolium (NBT) reduction. Clinica Chimica Acta 214(1):103-4. *https://doi.org/10.1016/0009-8981(93)90307-p*

Febres VJ, Fadli A, Meyering B, Yu F, Bowman KD, Chaparro JX, Albrecht U (2024). Dissection of transcriptional events in graft incompatible reactions of "Bearss" lemon (*Citrus limon*) and "Valencia" sweet orange (*C. sinensis*) on a novel citrandarin (*C. reticulata* × *Poncirus trifoliata*) rootstock. Frontiers in Plant Science 15:1421734. *https://doi.org/10.3389/fpls.2024.1421734*

Feng M, Augstein F, Kareem A, Melnyk CW (2024). Plant grafting: molecular mechanisms and applications. Molecular Plant 17(1):75-91. *https://doi.org/10.1016/j.molp.2023.12.006*

Fijalkowski KL, Kwarciak-Kozlowska A (2020). Phytotoxicity assay to assess sewage sludge phytoremediation rate using guaiacol peroxidase activity (GPX): a comparison of four growth substrates. Journal of Environmental Management 263:110413. *https://doi.org/10.1016/j.jenvman.2020.110413*

Fu Z, Jiao B, Nie B, Zhang G, Gao T (2016). A comprehensive generic-level phylogeny of the sunflower family: Implications for the systematics of Chinese Asteraceae. Journal of Systematics and Evolution 54(4):416-437. *https://doi.org/10.1111/jse.12216*

Gajjar P, Ismail A, Islam T, Darwish GA, Moniruzzaman M, Abuslima E, Sharkawy E I (2023). Physiological comparison of two salt-excluder hybrid grapevine rootstocks under salinity reveals different adaptation qualities. Plants 12(18):3247. *https://doi.org/10.3390/plants12183247*

Garcia LRL, Torres RV, Cortes GA, Villarreal MR, Jacome PRJ (2023). Effect of pepper rootstocks as a sustainable alternative to improve yield and fruit quality. Horticulturae 9(7):795. *https://doi.org/10.3390/horticulturae9070795*

Goldschmidt EE (2014). Plant grafting: new mechanisms, evolutionary implications. Frontiers in Plant Science 5:727. *https://doi.org/10.3389/fpls.2014.00727*

Jones CG, Daniel Hare J, Compton SJ (1989). Measuring plant protein with the Bradford assay: 1. evaluation and standard method. Journal of Chemical Ecology 15(3):979-92. *https://doi.org/10.1007/BF01015193*

Kawaguchi K, Notaguchi M, Okayasu K, Sawai Y, Kojima M, Takebayashi Y, ... Shiratake K (2024). Plant hormone profiling of scion and rootstock incision sites and intra- and inter-family graft junctions in *Nicotiana benthamiana*. Plant Signaling & Behavior 19(1). *https://doi.org/10.1080/15592324.2024.2331358*

Kováčik J, Klejdus B (2012). Tissue and method specificities of phenylalanine ammonia-lyase assay. Journal of Plant Physiology 169(13):1317-20. *https://doi.org/10.1016/j.jplph.2012.04.008*

Kumar A, Lakshmi V, Sangam S, Goswami TN, Kumar M, Akhtar S, Chattopadhyay T (2023). Marker assisted early generation identification of root knot disease resistant orange tomato segregants with multiple desirable alleles. Physiology and Molecular Biology of Plants 29(8):1179-1192. *https://doi.org/10.1007/s12298-023-01361-1*

Kurotani KI, Notaguchi M (2021). Cell-to-cell connection in plant grafting-molecular insights into symplasmic reconstruction. Plant Cell Physiology 62(9):1362-1371. *https://doi.org/10.1093/pcp/pcab109*

Li W, Chen X, Zhao S, Zhan Q, Chen S, Jiang J, ... Guan Z (2022). Effect of grafting on the growth and flowering of sprays chrysanthemums. Scientia Horticulturae 291. *https://doi.org/10.1016/j.scienta.2021.110607*

Liu Q, Wang X, Zhao Y, Xiao F, Yang Y (2023). Transcriptome and physiological analyses reveal new insights into delayed incompatibility formed by interspecific grafting. Scientific Reports 13(1):4574. *https://doi.org/10.1038/s41598-023-31804-4*

López Serrano L, Calatayud Á, Cardarelli M, Colla G, Rouphael Y (2022). Improving bell pepper crop performance and fruit quality under suboptimal calcium conditions by grafting onto tolerant rootstocks. Agronomy 12(7):1644-1644. *https://doi.org/10.3390/agronomy12071644*

Loupit G, Brocard L, Ollat N, Cookson SJ (2023). Grafting in plants: recent discoveries and new applications. Journal of Experimental Botany 74(8):2433-2447. *https://doi.org/10.1093/jxb/erad061*

Lupp RM, Marques DN, Lima Nogueira M, Carvalho MEA, Azevedo RA, Piotto FA (2024). Cadmium tolerance in tomato: determination of organ-specific contribution by diallel analysis using reciprocal grafts. Environmental Science and Pollution Research International 31(1):215-227. *https://doi.org/10.1007/s11356-023-31230-z*

Machin F, Hasbioğlu Y, Kragler F (2022). An *Arabidopsis* callus grafting method to test cell-to-cell mobility of proteins. Methods in Molecular Biology 2457:299-312. *https://doi.org/10.1007/978-1-0716-2132-5_20*

Matić P, Sabljić M, Jakobek L (2017). Validation of spectrophotometric methods for the determination of total polyphenol and total flavonoid content. Journal of AOAC International 100(6):1795-1803. *https://doi.org/10.5740/jaoacint.17-0066*

Mauro RP, Agnello M, Onofri A, Leonardi C, Giuffrida F (2020). Scion and rootstock differently influence growth, yield and quality characteristics of cherry tomato. Plants (Basel) 9(12):1725. *https://doi.org/10.3390/plants9121725*

Nie W, Wen D (2023). Study on the applications and regulatory mechanisms of grafting on vegetables. Plants (Basel) 12(15):2822. *https://doi.org/10.3390/plants12152822*

Notaguchi M, Kurotani KI, Sato Y, Tabata R, Kawakatsu Y, Okayasu K, ...Higashiyama T (2020). Cell-cell adhesion in plant grafting is facilitated by β-1,4-glucanases. Science 369(6504):698-702. *https://doi.org/10.1126/science.abc3710*

Pang Z, Cai Y, Xiong W, Xiao J, Zou J (2021). A spectrophotometric method for measuring permanganate index (COD Mn) by N,N-diethyl-p-phenylenediamine (DPD). Chemosphere 266:128936. *https://doi.org/10.1016/j.chemosphere.2020.128936*

Rashedy AA, Hamed HH (2023). Morphological, physio-biochemical and nutritional status as potential markers for grafting compatibility in Kalamata olive cultivar. BMC Plant Biology 23 (1):334. *https://doi.org/10.1186/s12870-023-04346-0*

Rondel C, Marcato-Romain CE, Girbal-Neuhauser E (2013). Development and validation of a colorimetric assay for simultaneous quantification of neutral and uronic sugars. Water Research 47(8):2901-8. *https://doi.org/10.1016/j.watres.2013.03.010*

Sharma A, Zheng B (2019). Molecular responses during plant grafting and its regulation by auxins, cytokinins, and gibberellins. Biomolecules 9(9):397. *https://doi.org/10.3390/biom9090397*

Shehata SA, Omar HS, Elfaidy AGS, El-Sayed SSF, Abuarab ME, Abdeldaym EA (2022). Grafting enhances drought tolerance by regulating stress-responsive gene expression and antioxidant enzyme activities in cucumbers. BMC Plant Biology 22(1):408. *https://doi.org/10.1186/s12870-022-03791-7*

Shi F,Jia X,Zhao C,Chen Y (2010). Antioxidant activities of various extracts from *Artemisisa selengensis* Turcz (LuHao). Molecules 5(7):4934-4946. *https://doi.org/10.3390/molecules15074934*

Skočajić D, Gašić U, Dabić Zagorac D, Nešić M, Tešić Ž, Meland M, Fotirić Akšić M (2021). Analysis of phenolic compounds for the determination of grafts (in) compatibility using *in vitro* callus cultures of Sato-Zakura cherries. Plants (Basel) 10(12):2822. *https://doi.org/10.3390/plants10122822*

Thippan S, Bunya-Atichart K, Ayuttaya S I N, Lerslerwong L (2024). Histological and biochemical aspects as potential markers for evaluation graft compatibility in durian at the early nursery stage. Scientia Horticulturae 337. *https://doi.org/10.1016/j.scienta.2024.113490*

Tsutsui H, Notaguchi M (2017). The use of grafting to study systemic signaling in plants. Plant Cell Physiology 58(8):1291-1301. *https://doi.org/10.1093/pcp/pcx098*

Tu Y (2016). Artemisinin-A gift from traditional Chinese medicine to the world (Nobel Lecture). Angewandte Chemie (International ed. in English) 55(35):10210-26. *https://doi.org/10.1002/anie.201601967*

Wang J, Han J, Lu Z, Lu F (2020). Preliminary structure, antioxidant and immunostimulatory activities of a polysaccharide fraction from *Artemisia selengensis* Turcz. International Journal of Biology Macromolecules 143:842-849. *https://doi.org/10.1016/j.ijbiomac.2019.09.145*

Wang L, Liao Y, Liu J, Zhao T, Jia L, Chen Z (2024). Advances in understanding the graft healing mechanism: a review of factors and regulatory pathways. Horticulture Research 11(8):uhae175. *https://doi.org/10.1093/hr/uhae175*

Wang S, Xie X, Zhang L, Hu Y, Wang H, Tu Z (2020). Inhibition mechanism of α -glucosidase inhibitors screened from *Artemisia selengensis* Turcz root. Industrial Crops & Products 143:111941. *https://doi.org/10.1016/j.indcrop.2019.111941*

Xu C, Wu F, Guo J, Hou S, Wu X, Xin Y (2022). Transcriptomic analysis and physiological characteristics of exogenous naphthylacetic acid application to regulate the healing process of oriental melon grafted onto squash. PeerJ 10:e13980. *https://doi.org/10.7717/peerj.13980*

Xu C, Zhang Y, Zhao M, Liu Y, Xu X, Li T (2021). Transcriptomic analysis of melon/squash graft junction reveals molecular mechanisms potentially underlying the graft union development. PeerJ 9:e12569. *https://doi.org/10.7717/peerj.12569*

Yildirim Hakan, Çalar Nazan, Onay Ahmet,Karlidag Hüseyin, Kan Tuncay (2017). *In vitro* micrografting of woody plant species-I (rootstock, scion, grafting technique). Journal of the Institute of Science and Technology 7(3):31-37. *https://doi.org/10.21597/jist.2017.158*

Zhang L, Tu Z, Yuan T, Wang H, Fu Z, Wen Q, Wang X (2014). Solvent optimization, antioxidant activity, and chemical characterization of extracts from *Artemisia selengnesis* Turcz. Industrial Crops & Products 56:223-230. *https://doi.org/10.1016/j.indcrop.2014.03.003*